



**HAL**  
open science

## A method for classifying and comparing non-linear trajectories of ecological variables

Stanislas Rigal, Vincent Devictor, Vasilis Dakos

► **To cite this version:**

Stanislas Rigal, Vincent Devictor, Vasilis Dakos. A method for classifying and comparing non-linear trajectories of ecological variables. *Ecological Indicators*, 2020, 112, pp.106113. 10.1016/j.ecolind.2020.106113 . hal-03051861

**HAL Id: hal-03051861**

**<https://hal.umontpellier.fr/hal-03051861v1>**

Submitted on 15 Dec 2020

**HAL** is a multi-disciplinary open access archive for the deposit and dissemination of scientific research documents, whether they are published or not. The documents may come from teaching and research institutions in France or abroad, or from public or private research centers.

L'archive ouverte pluridisciplinaire **HAL**, est destinée au dépôt et à la diffusion de documents scientifiques de niveau recherche, publiés ou non, émanant des établissements d'enseignement et de recherche français ou étrangers, des laboratoires publics ou privés.

# 1 **A method for classifying and comparing non-linear trajectories of ecological variables**

2

3 Stanislas Rigal<sup>1\*</sup>, Vincent Devictor<sup>1</sup>, Vasilis Dakos<sup>1</sup>.

4 <sup>1</sup>ISEM, Univ Montpellier, CNRS, EPHE, IRD, Montpellier, France.

5 \*Corresponding author, email: stanislas.rigal@umontpellier.fr

6

## 7 **Abstract**

8

9 Temporal dynamics in ecological variables are usually assessed using linear trends or smoothing  
10 methods. Those trends qualitatively summarise the increase or decrease in the variable of interest  
11 over a given time period. Yet, linear trends do not capture changes in the direction or in the rate of  
12 change of indices such as population trajectories, that may typically occur when conditions improve  
13 or worsen following conservation actions or environmental disturbances. In a similar way, non-  
14 linear methods while aiming to fully characterise population trajectories, fail to end up with a  
15 standard classification. Here, we propose and test a simple method to classify the trajectory of a  
16 given ecological variable according to its trend and acceleration. Our method is based on fitting a  
17 second order polynomial that is used to describe a trajectory according to its direction, velocity, and  
18 curvature (accelerated or decelerated). We apply this method to the temporal dynamics of bird  
19 populations monitored by the French Breeding Bird Survey as a case study. Using data for more  
20 than 100 species monitored from 1989 to 2017 in more than 2000 sites, we show that one quarter of  
21 the studied species have dynamics that can be better described by our polynomial approach than  
22 typically-used linear analysis. We also show how it can be used to analyse indicators constructed  
23 with multi-species indices. Our method can be applied to any type of ecological variable either to  
24 classify trajectories of ecological variables in time or trajectories of ecological variables across  
25 pressure gradients. Overall, our results suggest a more systematic investigation of non-linear  
26 trajectories when analysing the dynamics of ecological variables.

27

28 Key-words: bird, conservation, ecological variables, non-linearity, polynomials, population  
29 dynamics, trend analysis.

30

## 31 **1. Introduction**

32

33 As biodiversity is undergoing a major decline (Ripple *et al.*, 2017), international initiatives have set  
34 several ambitious targets to combat this trend, by protecting species and habitats or maintaining and  
35 restoring ecosystems (CBD, 2010; EC, 2011). These objectives require the development of relevant  
36 data and statistical tools to estimate any progress towards those targets.

37

38 Different types of variables has been proposed for measuring the “changing state of nature”. For  
39 instance, a suite of “biodiversity variables” have been proposed to detect critical biodiversity

40 changes (Schmeller *et al.* 2018). Whatever the ecological level considered (species, habitat,  
41 ecosystem) and the specific definition used (variable, indices, indicator), detecting changes in the  
42 dynamics of biodiversity responses is key to temporal ecology and conservation policy (Wolkovich  
43 *et al.*, 2014). Among possible approaches, the analysis of temporal trends in populations of habitat  
44 specialist species (*e.g.* farmland birds, Gregory *et al.*, 2005), or in aggregated indicators of  
45 population dynamics (*e.g.* Living Planet Index, Loh *et al.*, 2005) has become common practice for  
46 monitoring human impact on biodiversity (Vačkář *et al.* 2012).

47  
48 Ideally, an improved biodiversity status should be revealed by a switch from a decrease to an  
49 increase (or at least to a stabilisation) in the temporal trend of those indices (Donald *et al.*, 2007;  
50 Koleček *et al.*, 2014; Sanderson *et al.*, 2016; Koschová *et al.*, 2018). More generally, the aim of  
51 calculating temporal trends is to describe the state of a given variable with regard to its past with a  
52 straightforward descriptor that can be easily interpreted and used in further analysis (*e.g.* to compare  
53 dynamics between species or to relate the trend in the variable to specific pressures).

54  
55 However, the term "trend" creates confusion about what is measured when a statistical model is  
56 fitted to a trajectory (*i.e.* a time series) of a given variable of interest. The trend is usually measured  
57 after fitting a linear model that estimates the average rate of change of the variable over a given  
58 period (Link and Sauer, 1997a) and it is used to describe the trajectory. When estimating a trend,  
59 however, one only synthesises the overall change in terms of direction (the sign of the trend), and  
60 steepness (the magnitude of the trend). Yet, a trajectory is more than its trend as it is defined by the  
61 pattern of fluctuation itself. When studying a trajectory, the purpose should rather be to find the  
62 most accurate description of changes over time in terms of direction, velocity, curvature, or even the  
63 timing of such changes. Surprisingly, trends and trajectories are not always separated in the study of  
64 ecological variables (Humbert *et al.*, 2009; Inger *et al.*, 2014).

65  
66 Relying on linear trend methods or on a percentage of change between the first and last values  
67 remains largely dominant in classifying and comparing temporal changes in population dynamics  
68 for most of the well-studied groups, such as birds (Julliard *et al.*, 2004; Donald *et al.*, 2007; Reif,  
69 2013; Inger *et al.*, 2014; Heldbjerg *et al.*, 2018; Rosenberg *et al.*, 2019), fish (Christensen *et al.*,  
70 2014; Vasilakopoulos *et al.*, 2014), and insects (Hallmann *et al.*, 2017; Lister and Garcia, 2018;  
71 Sánchez-Bayo and Wyckhuys, 2019). But focusing either on trends or trajectories can lead to  
72 different interpretations as numerous population dynamics are non-linear (Clark and Luis, 2019) .  
73 Before any qualitative change of a given variable can be detected, the trajectory of the variable can  
74 adopt different shapes with specific meanings that cannot be captured by simply measuring the  
75 trend. For instance, for a population trajectory reflecting the conservation status of a threatened

76 species, the deceleration of the decrease already reveals a better situation (Fig. 1A). On the contrary,  
77 an accelerated decrease mirrors a stronger degradation (Fig. 1B). Thus, the variation in the rate of  
78 change along the trajectory is highly informative from a conservation perspective and yet cannot be  
79 entirely captured by a linear trend approach. Worse, linear trends can mask reversal dynamics, a  
80 concave or convex hump shaped curve that is typically qualified as “stable” by a linear model (Fig.  
81 1C). Therefore, studying complete trajectories beyond simple trends is crucial to track the  
82 improvement or failure in conservation policies as well as to identify changing points that may  
83 follow the implementation of a conservation policy.

84  
85 A plethora of other than linear methods to describe population trajectories is already available  
86 (Thomas, 1996; Link and Sauer, 1997b; Ruppert *et al.*, 2009; Dornelas *et al.*, 2013; Tittensor *et al.*,  
87 2014). Most of these methods rest on generalised linear models with polynomial regression splines  
88 (Cunningham and Olsen, 2009) or generalised additive models (GAM) (Fewster *et al.*, 2000;  
89 Buckland *et al.*, 2005). Although these methods are fundamental to fit and describe complex non-  
90 linear dynamics, the details of such complex shapes can be irrelevant for assessing the status of a  
91 population trajectory and difficult to use for comparison between different species. The reason is  
92 that in these non-linear models, the type of function used and the degree of freedom allocated to the  
93 corresponding statistical models are often not *a priori* constrained by the user (otherwise it would  
94 correspond to a parametric case (Brun *et al.* 2019)) but rather adjusted to the data. This leads to  
95 difficult interpretations as the risk of overfitting increases compromising the comparison between  
96 datasets. For instance in a GAM, smooth functions are built on a trade-off between the smoothness  
97 of the function and the fidelity to the data which implies a selection (either by generalised cross  
98 validation or marginal likelihood) of the smoothing parameters (Wood, 2017). Alternatively, simple  
99 non-parametric methods also exist (*e.g.* correlation rank (Yue and Wang, 2004; Sonali and Kumar,  
100 2013; Adarsh and Janga Reddy, 2015)), but they remain highly conservative in detecting no more  
101 than a dominant trend. Other methods identify breakpoints along a trajectory, for instance by fitting  
102 segmented relations usually through piecewise regression models (Muggeo, 2003; Muggeo, 2008;  
103 Fong *et al.*, 2017), or by applying sequential or iterative regime shift analysis methods (Rodionov  
104 and Overland, 2005; Gröger *et al.*, 2011). Although these techniques help to locate abrupt changes  
105 along a trajectory, they do not synthesise the trajectory beyond identifying particular changing  
106 points.

107  
108 Overall, the current approaches to study and compare non-linear trajectories in ecological variables  
109 do not offer a simple method for classifying trajectories based on their general shape. Such a  
110 method should be flexible enough to handle most ecological data, it should use simple statistical

111 estimates to classify trajectories, and these estimates should be easy-to-use for comparing different  
112 trajectories. We suggest that a method that meets these criteria could include: a) estimating the  
113 direction of change of a trajectory, b) estimating the rate of change of a trajectory, c) identifying  
114 whether the rate of change is accelerating or decelerating within a trajectory, and d) detecting points  
115 where the direction of change of a trajectory switches sign. Such a method would not reject linear  
116 trend analysis nor replaces GAM-like approaches, but would rather aim at providing a simple and  
117 generic classification of non-linear trajectories.

118  
119 In this paper, we develop such a generic method to classify trajectories of any ecological variable  
120 (population indices, multi-species indicators or any kind of temporal series) according to their  
121 direction (decline, increase, stable) as well as to their overall shape (accelerated, decelerated,  
122 convex or concave). We describe this method step-by-step and we test it in simulated trajectories  
123 that resemble typical time series of monitored populations. We further show how and why this  
124 method could be used in two empirical examples. We use population dynamics of the 108 most  
125 common species monitored by the French Breeding Bird Survey (FBBS) from 1989 to 2017 (Jiguet  
126 *et al.*, 2007) to illustrate how our method can be used to describe the conservation status of these  
127 populations. We finally apply this method on multi-species indicators (MSI) for farmland and  
128 woodland birds. We anticipate that this method will be sensitive to well identified pitfalls of  
129 classical monitoring programs (Buckland and Johnston, 2017) that might have a particular  
130 incidence on the uncertainty of the variable of interest resulting in a wider sampling error. A method  
131 accounting for this sampling error has been recently proposed for multi-species indicators (Soldaat  
132 *et al.*, 2017). We therefore adapted this method to take into account sampling error in our method  
133 when it is available. We also tested the sensitivity of our method to critical methodological choices  
134 or change in data quality. We highlight the advantages and disadvantages of our approach by  
135 comparing our results to those estimated by most common linear methods.

## 136 137 **2. Materials and methods**

### 138 139 2.1 A general classification of trajectories for ecological variables

140  
141 We use the properties of a second order polynomial function to describe and classify the overall  
142 shape of any trajectory.

143  
144 Let  $Y$  be a quantitative discrete or continuous variable (*e.g.* population abundance or any ecological  
145 variable) and  $X$  a quantitative continuous variable representing time (year, month or days). The  
146 characterisation of a second order polynomial function can be achieved in two steps (Fig. 2A):

147  
148 Step 1. We first fit a second order polynomial between  $Y$  and  $X$  through a least-square regression:

149

$$150 \quad Y = \alpha_0 + \alpha_1 X + \alpha_2 X^2 \quad (1)$$

151

152 Such a regression model performed using orthogonal polynomials removes the correlation between  
153 the first ( $X$ ) and the second order ( $X^2$ ) variables (Narula, 1979). The significance of each coefficient  
154 ( $\alpha_1$  for first order and  $\alpha_2$  for second order) is therefore used to test whether the second order  
155 significantly improves the regression compared to the first order. More precisely, a second order  
156 polynomial (Eq. 1) can discriminate between a stationary process (if  $\alpha_1$  and  $\alpha_2$  are not significant), a  
157 monotonous process (if only  $\alpha_1$  is significant), and an accelerated process (if  $\alpha_2$  is significant).

158

159 We fit this function within the interval bounded by  $X_0$  and  $X_T$ , respectively the first and last values  
160 of  $X$ , to generate a curve that can be either convex ( $\cup$ ) or concave ( $\cap$ ) (Fig. 3). For a convex curve,  
161 this interval on which the function is fitted necessarily delineates one of the following cases: a  
162 decelerated decline (Fig. 3A.1), a convex phase (Fig. 3A.2) or an accelerated increase (Fig. 3A.3).  
163 For a concave case three analogous cases can be described: a decelerated increase (Fig. 3B.1), a  
164 concave phase (Fig. 3B.2), or an accelerated decline (Fig. 3B.3).

165

166 Step 2. We then characterise the fitted polynomial function with simple metrics, *i.e.* we transform  
167 the information contained within the function and the interval into a readable description using the  
168 direction, the acceleration, the velocity and the changing points of the trajectory (Fig. 2-3). The  
169 direction of the trajectory is defined as being either a decline, nil or an increase. The acceleration  
170 corresponds to an accelerated, constant, or decelerated phase when the direction is either a decline  
171 or an increase, or refers to a convex, stable or concave phase when there is no direction (Fig. 2).  
172 Moreover, the velocity represents the rate of change of a given trajectory and the changing points  
173 designate where the rate of change of the trajectory adopts a different profile (Fig. 3).

174

175 For linear cases ( $\alpha_2$  non significant),  $Y$  becomes a linear function of  $X$  (*i.e.*  $Y = \alpha_0 + \alpha_1 X$ ). The four  
176 indices are completely determined by the sign and the magnitude of the slope ( $\alpha_1$ ). The direction is  
177 an increase, nil, or a decline for positive, null, or negative slopes respectively. The acceleration is  
178 null, the velocity is the magnitude of the slope and there is no specific point of noticeable change  
179 that can be identified.

180

181 For non-linear cases ( $\alpha_2$  significant), a standardised classification should be able to discriminate  
 182 between decelerated or accelerated cases and convex, stable or concave dynamics (Fig. 3). This is  
 183 done as follows:

184

185 Direction. To qualify the behaviour of the function over a given period, we use the direction of the  
 186 function around the centre  $X_m$  of the interval  $[X_0, X_T]$  (corresponding to the whole time series  
 187 length). The direction of  $Y$  is then determined by the sign of the slope of the tangent  $T_{X_m}$  given by  
 188 the linearisation around  $X_m$ :

189

$$190 \quad T_{X_m}(X) = \dot{Y}(X_m)(X - X_m) + Y(X_m) \quad (2)$$

191

192 where  $\dot{Y}(X_m)$  is the first derivative of  $Y$ :

193

$$194 \quad \dot{Y}(X_m) = \alpha_1 + 2\alpha_2 X_m \quad (3)$$

195

196  $\dot{Y}$  is computed around  $X_m$  both at  $X_m - \delta$  and  $X_m + \delta$  (Fig. 3), where  $\delta$  is equal to 25% of the interval  
 197  $[X_0, X_T]$ . As the direction can change only once along a second order polynomial, if this  
 198 modification does not happen on  $[X_m - \delta, X_m + \delta]$ , it implies that the change occurs either on  $]-\infty, X_m - \delta[$   
 199 or on  $]X_m + \delta, +\infty[$ . If it occurs on  $]-\infty, X_m - \delta[$ , the direction is constant on  $[X_m - \delta, X_T]$  and by symmetry,  
 200 if the change happens on  $]X_m + \delta, +\infty[$ , the direction is constant on  $[X_0, X_m + \delta]$ . In both cases, the  
 201 direction stays the same on at least 75% of the interval  $[X_0, X_T]$  and we assume this direction  
 202 accurately reflects the main direction of  $Y$  on  $[X_0, X_T]$ . In these cases, if  $\dot{Y}(X_m - \delta) > 0$  and  $\dot{Y}(X_m + \delta) >$   
 203  $0$ , the direction is an increase and if  $\dot{Y}(X_m - \delta) < 0$  and  $\dot{Y}(X_m + \delta) < 0$ , the direction is a decline. If the  
 204 sign of  $\dot{Y}$  changes on the interval  $[X_m - \delta, X_m + \delta]$ , it means that  $\dot{Y}$  becomes zero around  $X_m$  and hence  
 205 the direction is considered as nil and there is no alternative possibility.

206

207 Acceleration. The acceleration of the polynomial fit on the interval is given either by the sign of the  
 208 second order coefficient  $\alpha_2$  or by the sign of  $\dot{\gamma}$ , the derivative of the curvature function  $\gamma$  (Eq. 4)  
 209 (O'Neill, 2006). This choice depends on whether the direction is nil (sign of  $\dot{Y}(X_m - \delta) \neq$  sign of  
 210  $\dot{Y}(X_m + \delta)$ ) or not.

211

$$\dot{\gamma}(X_m) = \frac{-12\alpha_2^2(2\alpha_2 X_m + \alpha_1)}{(1 + (2\alpha_2 X_m + \alpha_1)^2)^{\frac{5}{2}}} \quad (4)$$

213

214 When the direction is nil (Fig. 3 A.2, B.2), the acceleration refers to the convexity or concavity of  
 215 the trajectory and only the sign of  $\alpha_2$  is needed to describe it (convex for  $\alpha_2 > 0$ , concave  $\alpha_2 < 0$ ).  
 216 When the direction is an increase or decline (Fig. 3 A.1, A.3, B.1 and B.3), the acceleration cannot  
 217 be described solely by the sign of  $\alpha_2$ , because whether the function is in an accelerated or  
 218 decelerated phase depends on the interval which is regarded. For instance, if  $\alpha_2 > 0$ , we could have  
 219 a decelerated decline (Fig. 3A.1) or an accelerated increase (Fig. 3A.3) depending on the interval  
 220 considered. We therefore introduce a criterion that directly refers to the curvature  $\dot{\gamma}$  of the function  
 221 irrespective of the interval (Fig. S1). This criterion is given by computing  $\dot{\gamma}$  the first derivative of  
 222 the curvature function  $\gamma$  at  $X_m$  the centre of the interval  $[X_0, X_T]$  (Eq. 4) (supplementary materials 1  
 223 for calculation details).

224

225 When the interval is on the left side of the minimum or maximum of the second order polynomial,  
 226 whatever the sign of  $\alpha_2$ , the function is decelerating (Fig. S1). When the interval is on the right side  
 227 of the minimum or maximum, the function shows an acceleration. The sign of  $\dot{\gamma}$  is the opposite  
 228 when the sign of  $\alpha_2$  changes. By multiplying the sign of  $\dot{\gamma}$  by the sign of  $\alpha_2$ , we obtain a consistent  
 229 type of acceleration for the variable considered ( $Y$ ). When this sign is negative, it corresponds to an  
 230 acceleration and when it is positive, it corresponds to a deceleration.

231

232 Velocity. The velocity is given by the magnitude of the tangent at  $X_m$ , *i.e.* the value of  $\dot{Y}(X_m)$  (Eq. 3).  
 233 The velocity can be compared between two curves only if they belong to the same type of  
 234 trajectories. For instance, it would not make sense to compare the speed of a decelerated trajectory  
 235 (Fig 2B case 9) with the speed (slope) of a linear increase (Fig 2B case 6).

236

237 Changing points. Non-linear or multiple linear regression methods can provide changing points or  
 238 periods (Buckland *et al.*, 2005; Fewster *et al.*, 2000; Muggeo, 2003; Cunningham and Olsen, 2008;  
 239 Smith *et al.*, 2015). Here, for each second order polynomial curve three local points of interest can  
 240 be identified in theory. Those points correspond to values of  $X$  where a shift in the rate of change is  
 241 observed. No significance test is required as the significance of the second order polynomial implies  
 242 the existence of these points (but see below for standard deviation). The first point ( $p_1$ ) marks the



243 minimum (for convex cases) or maximum (for concave cases) of the polynomial curve and  
 244 corresponds to the value of  $X$  when  $\dot{Y}$  is zero (Eq. 5). The two other points ( $p_2$  and  $p_3$ ) delineate the  
 245 values of  $X$  where the rate of change is mainly driven by a horizontal or vertical component (Eq. 6)  
 246 (see supplementary material 2). In practice, among these three points ( $p_1$ ,  $p_2$  and  $p_3$ ), only the ones  
 247 which fall within the interval  $[X_0, X_T]$  are generally relevant (Fig. 3). These points only serve as  
 248 potential changing points in the overall shape of trajectories and need to be interpreted as such by  
 249 the user.

250

$$251 \quad \begin{cases} \dot{Y}(p_1) = \alpha_1 + 2\alpha_2 p_1 \\ \dot{Y}(p_1) = 0 \end{cases} \Rightarrow p_1 = \frac{-\alpha_1}{2\alpha_2} \quad (5)$$

$$252 \quad \begin{cases} \dot{Y}(p_2) = -1 \\ \text{or} \\ \dot{Y}(p_3) = 1 \end{cases} = \begin{cases} p_2 = \frac{-\alpha_1 + 1}{2\alpha_2} \\ \text{or} \\ p_3 = \frac{-\alpha_1 - 1}{2\alpha_2} \end{cases} \quad (6)$$

253

254 In many cases, the sampling error of the  $Y$  value is also accessible and needs to be considered to  
 255 estimate  $Y$  uncertainty. We therefore use a Monte Carlo simulation method to account for this  
 256 sampling error (SE) adapted from Soldaat *et al.* (2017). We first set the  $Y$  value for the reference  
 257 year (baseline year that can be either the first, last or central year or a specific year chosen by the  
 258 user) to 100 and any  $Y$  value below 1 is truncated to 1 and its SE set to 0. We then log-transformed  
 259 the  $Y$  values and we applied the Delta-method (Agresti, 2002) to obtain the sampling error of  $Y$  on a  
 260 log scale ( $SE_{\log}(Y) = SE(Y)/Y$ ). 1000  $Y$  vectors are then simulated by taking values from a normal  
 261 distribution with a mean equal to the log-transformed  $Y$  values and the standard deviation equal to  
 262 the  $SE_{\log}$ . Each  $Y$  vector is back-transformed to the original  $Y$  scale, the reference year value is set to  
 263 100 and other values are expressed as a percentage of the value of the reference year. We then  
 264 classify each simulated  $Y$  after estimating its acceleration, velocity and potential changing points.  
 265 As simulated trajectories may be classified in different classes, we perform a binomial (if two  
 266 different classes) or multinomial (if more than two different classes) test to assess the significance  
 267 of the predominant class. If both a non-linear and a linear class are predominant but none of them  
 268 significantly,  $Y$  is classified as belonging to the linear class. Only the simulations belonging to the  
 269 selected class are kept and used to calculate the average velocity and the average changing points (if  
 270 any) and their standard deviation.

271

272 In summary, using the classification method described above (Fig. 2A), one can classify any  
273 trajectory as belonging to only one of the nine classes: accelerated decline, constant decline,  
274 decelerated decline, concave, stable, convex, decelerated increase, constant increase and accelerated  
275 increase (Fig. 2B). The direction and the type of acceleration are enough to cover this classification  
276 which is obtained unambiguously because both the direction and the acceleration are retrieved from  
277 the statistical significance of the second order polynomial coefficients. Moreover, two additional  
278 properties can be easily obtained, namely the velocity of the change, and potential changing point(s)  
279 with a significant shift in the rate of change of Y. The classification being based on trajectories in a  
280 given interval  $[X_0, X_T]$ , it is by definition dependent on the time interval considered. The  
281 incorporation of the sampling error allows to test the significance of the classification and to give an  
282 estimate of uncertainty (as standard deviation) for velocity and potential changing points.

283

## 284 2.2 Sensitivity to time series length, missing data, noise and sampling error

285

286 We tested the sensitivity of the proposed method on simulated trajectories that mimic each of the  
287 nine classes (Fig. 2B). To produce time series we used the second order polynomial (Eq. 1) with  
288 parameter values  $\alpha_1$  and  $\alpha_2$  chosen to be close to the coefficients obtained from empirical time  
289 series and selecting only the part of the produced parabola that resembled the nine classes (for  
290 details see supplementary material 3). We performed a sensitivity analysis to four potential sources  
291 of biases (see supplementary material 4). First, we explored the effect of the time series length.  
292 Second, we explored the effect of gaps in the monitored data as typically the frequency of  
293 monitoring can differ from year to year. Third, we explored the effect of process noise (Dennis *et*  
294 *al.*, 2006) as additional year-to-year variation on the trend. Noise corresponds to a deviation from  
295 the process and it influences the position of the Y value for a given X value. Finally, we explored the  
296 effect of sampling error due to incomplete sampling, weaknesses in detectability or  
297 misidentification of species. Sampling error corresponds to a dispersion metric of uncertainty of a Y  
298 value for a given X value.

299

## 300 2.3 Classifying trajectories of empirical ecological variables: an illustration using bird populations

301

302 We tested our method on an empirical dataset. We classified bird population time series from the  
303 French Breeding Bird Survey (FBBS) from 1989 to 2017. To be validated by the FBBS, volunteer  
304 ornithologists had to follow a standardised protocol on fixed sites (2693 since 1989) on which a  
305 fixed number of point counts were carried out by the same observer in the same order. Each point

306 count of each site is monitored twice a year during the same period (5 or 15 minutes) 1 to 4 hours  
307 after sunrise, between 1st of April and 15th of June to take into account early and late breeding  
308 birds. Of the 242 species recorded in the dataset, we selected the most abundant species (99% of the  
309 total abundance) to restrict our analysis only to the most common species, easy to observe and less  
310 exposed to sampling biases. After removing non-selected species and sites only monitored once, our  
311 dataset comprised 2144 sites and 108 species (supplementary materials 5). For each site and  
312 species, count data from all the points of each given site were summed (after taking the maximum  
313 of the two monitoring spring sessions for each point) as a proxy for the local abundance of the  
314 species in a given site and a given year.

315

316 Note that many ecological data are similar to what is collected by the FBBS, *i.e.* they use multi-  
317 species and multi-sites surveys to derive yearly variations in the abundance of each species or in  
318 more elaborated indicators combining multi-species indices (Loh *et al.*, 2005; Pereira and Cooper,  
319 2006; Butchart *et al.*, 2010; Inger *et al.*, 2014).

320

321 We thereafter applied our method to yearly population indices (see supplementary materials 6) of  
322 each of the 108 species from the FBBS during the period 1989-2017 corresponding to  $[X_0, X_T]$ ,  
323 using 2001 as the reference year. For each species  $i$ , the yearly index ( $Y_i$ ) was considered as the  
324 response variable ( $Y$ ) and years as polynomial explanatory variable ( $X$ ) (Eq. 1).

325

326 Finally, we also tested our method on multi-species indicators (MSI) rather than individual species.  
327 MSI are typically used to capture the general trend of a specific group of species of interest (*e.g.*  
328 farmland birds). To compile these MSI, we selected farmland and woodland specialist species  
329 (MNHN, 2019).

330

331 All analyses were performed in R (version 3.4.4). Bird data were obtained from the French National  
332 Natural History Museum in 2018. A workflow of the proposed method is available as Rmd file and  
333 can be downloaded at <https://github.com/StanislasRigal/classtrajjectory>.

334

### 335 **3. Results**

336

#### 337 3.1 General case

338

339 Testing our method on the simulated trajectories, we were able to correctly classify between 44.6%  
340 and 98.3% depending on the biases considered (Table 1). In terms of sensitivity to time series

341 length, we found that the classification was weakly sensitive to the length with a slightly better  
 342 classification percentage for longer time series (Table 1). 96.8% of the simulations were correctly  
 343 classified, when the time series length was 30, which is the time series length covered in the  
 344 empirical example. This percentage is not significantly different from the percentage obtained for  
 345 length equal to 70 (binomial test p-value = 0.156) but it was significantly higher than the percentage  
 346 obtained for a length equal to 10 (binomial test p-value < 0.0001). The highest percentage was  
 347 found for a length of 50 but it was not significantly higher than the percentage found for a length of  
 348 70 or 90 (binomial test p-value = 0.127 and 0.331). Overall this source of bias has less impact on  
 349 the percentage of correct classifications than others. The average distance between expected and  
 350 observed potential changing points was around 5 or 6% of the time series length. For missing data,  
 351 we found that the more the data are complete (the more the ratio between monitored years and time  
 352 series length is close to 1), the more the classifications were correct, with a maximum of 96.8% of  
 353 correct classification for a complete time series (ratio = 1). For noise and sampling error, we found  
 354 that these biases generated the most high percentage of misclassification.

355

<b>Time series length</b> (Years) (ratio of missing data = 1, noise = 5%, sampling error = 5%)	10	30	50	70	90
Correct classifications (%)	90.3	96.8	98.3	97.5	97.8
Mean relative distance from observed to simulated changing points (% of time series length)	4.9	5.0	5.5	5.8	6.3
<b>Missing data</b> (Ratio between monitored years and time series length) (time series length = 30, noise = 5%, sampling error = 5%)	0.2	0.4	0.6	0.8	1
Correct classifications (%)	48.8	59.7	72.5	82.8	96.8
Mean relative distance from observed to simulated changing points (% of time series length)	3.8	3.7	3.6	3.8	5.0
<b>Noise</b> (% of Y range) (time series length = 30, ratio of missing data = 1, sampling error = 5%)	5	15	25	35	45
Correct classifications (%)	96.8	82.4	63.3	48.9	44.6
Mean relative distance from observed to simulated changing points (% of time series length)	5.0	9.5	12.1	16.1	17.9
<b>Sampling error</b> (% of Y range) (time series length = 30, ratio of missing data = 1, noise = 5%)	5	15	25	35	45
Correct classifications (%)	96.8	85.6	56.8	54.8	51.7

Mean relative distance from observed to simulated changing points (% of time series length)	5.0	8.6	7.7	8.6	10.2
---	-----	-----	-----	-----	------

Table 1: Averaged percentages of correct classifications for each value of each source of bias. The time series length is expressed in years. The ratio corresponds to the number of monitored time steps to number of time steps. The process noise and the sampling error are expressed in percentage of the  $Y$  range ( $Y_{max}-Y_{min}$ ).

356

### 357 3.2 Case-study

358

359 We applied our classification method on bird population trajectories recorded in France from 1989  
 360 to 2017. We found that among the 108 species trajectories, 80 were linear while for the other 28  
 361 (*i.e.* 26% of the 108 trajectories) a second order polynomial was better than the linear fit. 26 species  
 362 trajectories were classified as increase of which three were decelerated and 23 constant (Fig. 4 F, I).  
 363 29 species trajectories were classified as decline of which four were decelerated, 24 constant and  
 364 one accelerated (Fig. 4 A, D, G). 53 species trajectories were neither classified as decline nor as  
 365 increase, of which four were convex, 33 remained stable and 16 had concave dynamics (Fig. 4 B, E,  
 366 H).

367

368 We also quantitatively compared trajectories based on their velocity. Note that the velocity was not  
 369 recorded when the trajectory direction was nil (concave, stable or convex classes) as it would have  
 370 been null. Also no velocity was calculated for the accelerated increase class as we found no species  
 371 belonging to this class. We found that species from the same class can differ greatly in velocity. For  
 372 instance, between two decelerated and declining species, *Pica pica* had a velocity three times greater  
 373 than *Corvus frugilegus* (respectively -8.4 and -3.0) depicting a stronger decrease of *Pica pica*  
 374 relative to *Corvus frugilegus*. Note that the comparison of species velocities for trajectories  
 375 belonging to different classes is not meaningful. For instance, the velocity of *Emberiza citrinella*, an  
 376 accelerated and declining species, is similar to the velocity of *Pica pica*, a decelerated and declining  
 377 species (respectively -9.2 and -8.4). The trajectories of those two species being different, their  
 378 velocities cannot be compared although they are quantitatively similar. This highlighted the need of  
 379 considering the trajectory class before conducting velocity comparisons and more generally the  
 380 need of caution when performing linear trend comparisons.

381

382 For some cases, we also detected potential changing points that depict either a change from an  
 383 increase to a decline (or *vice versa*), or an acceleration or deceleration of the rate of change. For

384 instance, *Emberiza citrinella* started to strongly decrease in 2007 ( $p_2$ ,  $sd = 1.9$ , Fig. 4A). During the  
385 same period, *Coloeus monedula* slowed down its decline in 1991 ( $p_2$ ,  $sd = 2.5$ ), reached a minimum  
386 in 2000 ( $p_1$ ,  $sd = 0.9$ ) and mainly increased after 2010 ( $p_3$ ,  $sd = 1.3$ ) (Fig. 4B). These points can  
387 provide additional information on each species dynamics of potential conservation interest such as  
388 population responses to pressure or conservation changes.

389

390 Using our method on MSI, we found a significant accelerated decline in farmland specialists (Fig.  
391 5A) ( $\alpha_2 = -0.08$ ,  $\alpha_1 = 300$ ,  $sd = 7.06$ ,  $p\text{-value} < 0.0001$ ). In contrast, we found a stable trend in  
392 woodland specialists (slope = 0.09,  $sd = 5.9$ ,  $p\text{-value} = 0.28$ ) (Fig. 5B).

393

#### 394 4. Discussion

395

396 In this paper, we showed how trajectories of ecological variables can be classified into nine classes  
397 using a method that is simply based on fitting a 2<sup>nd</sup> order polynomial model (Fig. 2). Our method  
398 basically dissects the dominant shape of a trajectory into 2 properties: the direction and the  
399 acceleration. In addition, this method can indicate the velocity and potential changing points along  
400 the trajectory where a shift in the rate of change happens. As such, our approach helps to provide  
401 comparable and easy-to-use information that goes beyond the current classification and comparison  
402 method based on linear trend analysis or percentage of change (Vorisek *et al.*, 2010; Inger *et al.*,  
403 2014).

404

405 When applied to empirical population trajectories, we showed how this method gives additional  
406 information on species dynamics compared to common linear approaches. Studying linear trends of  
407 our empirical example would have masked significant non-linear dynamics for more than 25% of  
408 the studied species between 1989 and 2017. Thus, using a common linear approach no distinction  
409 could have been found between species with stable trajectories and those with convex or concave  
410 dynamics, compared to fitting a second order polynomial function. Moreover, decreasing or  
411 increasing trends would only have been differentiated quantitatively using velocity whatever their  
412 individual shapes. Finally, potential changing points would have been inaccessible using a unique  
413 linear regression although they can be provided using other methods (Fewster *et al.*, 2000; Muggeo,  
414 2003; Cunningham and Olsen, 2009; Smith *et al.*, 2015). These remarks also stand for the multi-  
415 species indicators analysed in this study. The dynamic of the forest species MSI was classified as  
416 stable and other non-linear methods may be then applied to more precisely fit the narrow range  
417 variations. The dynamic of the farmland species MSI was categorised as an accelerated decline.

418 Therefore, beyond the now well-described decline in farmland birds (Donald *et al.*, 2001; Gregory  
419 *et al.*, 2019; Newton, 2004; Reif and Vermouzek, 2019), their decrease was even faster between  
420 1989 and 2017 in France. Of course, an analysis restricted to a different interval, like for instance  
421 focused on the last years (showing a stabilisation), would have led to a different classification.  
422 Thus, it should be clear that the classification given by this method synthesises the shape of the  
423 trajectory over the whole available time series. In that sense, different dynamics during a particular  
424 part of the trajectory may be explored by applying the method to a specific period.

425

426 The presented method can also be used to search for signs of improvement following, for instance,  
427 large-scale conservation policies. As pressures on ecosystems are not intrinsically supposed to be  
428 linear it may be relevant to combine this method to synthetically describe population trajectories  
429 along with non-linear dynamics of pressures that are experienced by species in different areas (*e.g.*  
430 to test whether the trajectories of ecological variables and of candidate pressures are similar (in  
431 shape) and synchronous (via the changing points)). Previous studies have selected a given year  
432 (often close to a new conservation legislation enforcement) to compute before/after linear trends or  
433 linear approximations (Donald *et al.*, 2007; Mace *et al.*, 2010; Koleček *et al.*, 2014; Sanderson *et*  
434 *al.*, 2016). Our method does not require the selection of a particular year. Rather, it can  
435 independently highlight specific points where trajectories change in direction, which can be used for  
436 evaluating a potential temporal lag between legislation and biodiversity responses (Male and Bean,  
437 2005).

438

439 The classification method we propose is sensitive, to some extent, to the length of the time series,  
440 the data resolution, the magnitude of noise (distance to the process influencing the position of a  
441 value) and the importance of sampling error (dispersion metric corresponding to the uncertainty of a  
442 value). The length of the time series does not influence a lot the quality of the classification above a  
443 minimal length. In suboptimal conditions (no missing data, weak noise and low sampling error),  
444 even for 10 year long time series, correct classification rate was high (90% see Table 1) and the  
445 changing points were set with a high accuracy. Gaps in the data may have a stronger influence on  
446 the classification due to a higher uncertainty for the polynomial fit. However for multi-species  
447 indicators the issue of missing years can be tackled using for instance chain indexing (Crawford *et*  
448 *al.*, 1991; Soldaat *et al.*, 2017). The noise on the process one wants to study remains difficult to  
449 estimate in empirical data, but its impact on correct classification ratio is confined to very noisy  
450 data (below two third of correct classification when the noise is higher than 25% of the index  
451 range). Finally, sampling error can be incorporated in our method to produce a more reliable

452 classification by allowing to test the significance of the class quantified as standard deviation for the  
453 polynomial coefficients and the changing points. High sampling error results in a more conservative  
454 classification as the significance of second order weakens. However, the accuracy of the  
455 classification remains high (above 85%) for most of the sampling error levels observed in our  
456 empirical example. When the data resolution or the length of the time series results in too few data  
457 available to fit a second order polynomial, a non-parametric alternative approach can be adopted to  
458 provide a similar classification using the correlation rank given by the Mann-Kendall test  
459 (supplementary materials 7). Such a non-parametric method is always less powerful (less sensitive  
460 to small changes) than the parametric one, but it can outperform the linear approach for low data  
461 resolutions (Table S1).

462

463 Although we focused on classifying population trajectories, we showed that our method can be  
464 applied to multi-species indicators. Trajectories of basically any type of ecological variable can also  
465 be classified using our method because fitting a second order polynomial does not require long and  
466 high-resolution data and it does not need any *a priori* parameter specifications, contrary to highly-  
467 parametric models as GAMs (Fewster *et al.*, 2000). These characteristics justify the flexibility of  
468 the method that allows it to be used with different types of ecological data, while keeping enough  
469 simplicity to obtain a meaningful classification of trajectories. Obviously, in cases where a full  
470 description of a trajectory is necessary or trajectories are highly non-linear, other existing methods  
471 will be more appropriate. In that sense, our proposed method does not replace linear and highly-  
472 descriptive approaches, but rather offers a complementary alternative by providing a classification  
473 for non-linear cases well adapted for tracking a wide variability of ecological variables including  
474 multi-species indicators (Gregory *et al.*, 2005; Collen *et al.*, 2009; Gregory and Van Strien, 2010;  
475 Brereton *et al.*, 2011; Rosenberg *et al.*, 2019) to inform and evaluate conservation actions.

476

#### 477 **Acknowledgements**

478 We warmly thank volunteers contributing to the FBBS. This project was funded by the ANR project  
479 DEMOCOM. We also thank two anonymous reviewers for their helpful comments.

480

481 Declarations of interest: none

482

#### 483 **References**

484



485 Adarsh, S., Janga Reddy, M. (2015). Trend analysis of rainfall in four meteorological subdivisions  
486 of southern India using nonparametric methods and discrete wavelet transforms. *Int. J. Climatol.*,  
487 35, 1107–1124. DOI: 10.1002/joc.4042  
488

489 Agresti, A., (2002). *Categorical data analysis*. John Wiley & Sons, Inc., Hoboken, New Jersey.  
490

491 Brereton, T., Roy, D. B., Middlebrook, I., Botham, M., Warren, M. (2011). The development of  
492 butterfly indicators in the United Kingdom and assessments in 2010. *J. Insect. Conserv.*, 15(1-2),  
493 139-151. DOI: 0.1007/s10841-010-9333-z  
494

495 Brun, P., Zimmermann, N. E., Graham, C. H., Lavergne, S., Pellissier, L., Münkemüller, T., &  
496 Thuiller, W. (2019). The productivity-biodiversity relationship varies across diversity dimensions.  
497 *Nat. Commun.*, 10(1), 1-11. DOI: 10.1038/s41467-019-13678-1  
498

499 Buckland, S.T., Magurran, A.E., Green, R.E., Fewster, R.M. (2005). Monitoring change in  
500 biodiversity through composite indices. *Philos. Trans. R. Soc. B Biol. Sci.*, 360, 243–254. DOI:  
501 10.1098/rstb.2004.1589  
502

503 Buckland, S.T., Johnston, A. (2017). Monitoring the biodiversity of regions: Key principles and  
504 possible pitfalls. *Biol. Conserv.*, 214, 23–34. DOI: 10.1016/j.biocon.2017.07.034  
505

506 Butchart, S.H., Walpole, M., Collen, B., Van Strien, A., Scharlemann, J.P., Almond, R.E., ... Bruno,  
507 J. (2010). Global biodiversity: indicators of recent declines. *Science*, 328(5982), 1164-1168. DOI:  
508 10.1126/science.1187512  
509

510 CBD. (2010). *The strategic plan for biodiversity 2011–2020 and the Aichi biodiversity targets*.  
511 *Convention on Biological Diversity Secretariat, Montreal*.  
512

513 Christensen, V., Coll, M., Piroddi, C., Steenbeek, J., Buszowski, J., Pauly, D. (2014). A century of  
514 fish biomass decline in the ocean. *Mar. Ecol. Prog. Ser.*, 512, 155–166. DOI: 10.3354/meps10946  
515

516 Clark, T. J., & Luis, A. D. (2019). Nonlinear population dynamics are ubiquitous in animals. *Nature*  
517 *Ecol. & Evol.*, 1-7. DOI: 10.1038/s41559-019-1052-6  
518

519 Collen, B. E. N., Loh, J., Whitmee, S., McRAE, L., Amin, R., Baillie, J. E. (2009). Monitoring  
520 change in vertebrate abundance: the Living Planet Index. *Conserv. Biol.*, 23(2), 317-327. DOI:  
521 10.1111/j.1523-1739.2008.01117.x  
522

523 Crawford, T. J. (1991). The calculation of index numbers from wildlife monitoring data. In  
524 *Monitoring for conservation and ecology* (pp. 225-248). Springer, Dordrecht. DOI: 10.1007/978-94-  
525 011-3086-8\_12  
526

527 Cunningham, R., Olsen, P. (2009). A statistical methodology for tracking long-term change in  
528 reporting rates of birds from volunteer-collected presence-absence data. *Biodivers. Conserv.*, 18,  
529 1305–1327. DOI: 10.1007/s10531-008-9509-y  
530

531 Dennis, B., Ponciano, J. M., Lele, S. R., Taper, M. L., Staples, D. F. (2006). Estimating density  
532 dependence, process noise, and observation error. *Ecol. Monogr.*, 76(3), 323-341. DOI:  
533 10.1890/0012-9615(2006)76[323:EDDPNA]2.0.CO;2  
534

535 Donald, P. F., Green, R. E., Heath, M. F. (2001). Agricultural intensification and the collapse of  
536 Europe's farmland bird populations. *Proc. R. Soc. B Biol. Sci.*, 268(1462), 25-29. DOI:  
537 10.1098/rspb.2000.1325  
538

539 Donald, P.F., Sanderson, F.J., Burfield, I.J., Bierman, S.M., Gregory, R.D., Waliczky, Z. (2007).  
540 International conservation policy delivers benefits for birds in Europe. *Science*, 317(5839), 810–  
541 813. DOI: 10.1126/science.1146002  
542

543 Dornelas, M., Magurran, A.E., Buckland, S.T., Chao, A., Chazdon, R.L., Colwell, R.K., ... Kosnik,  
544 M.A. (2013). Quantifying temporal change in biodiversity: challenges and opportunities. *P. Roy.  
545 Soc. B-Biol. Sci.*, 280(1750), 20121931. DOI: 10.1098/rspb.2012.1931  
546

547 EC. (2011). Our life insurance, our natural capital: an EU biodiversity strategy to 2020 (accessed  
548 10.30.18).  
549

550 Fewster, R.M., Buckland, S.T., Siriwardena, G.M., Baillie, S.R., Wilson, J.D. (2000). Analysis of  
551 population trends for farmland birds using generalized additive models. *Ecology*, 81(7), 1970–1984.  
552 DOI: 10.1890/0012-9658(2000)081[1970:AOPTFF]2.0.CO;2

553

554 Fong, Y., Huang, Y., Gilbert, P.B., Permar, S.R. (2017). chngpt: threshold regression model  
555 estimation and inference. *BMC Bioinformatics* 18, 454. DOI: 10.1186/s12859-017-1863-x

556

557 Gregory, R.D., Van Strien, A., Vorisek, P., Gmelig Meyling, A.W., Noble, D.G., Foppen, R.P.,  
558 Gibbons, D.W. (2005). Developing indicators for European birds. *Philos. Trans. Royal Soc. B-Biol.*  
559 *Sci.*, 360(1454), 269–288. DOI: 10.1098/rstb.2004.1602

560

561 Gregory, R. D., Van Strien, A. (2010). Wild bird indicators: using composite population trends of  
562 birds as measures of environmental health. *Ornithol. Sci.*, 9(1), 3-22. DOI: 10.2326/osj.9.3

563

564 Gregory, R.D., Skorpilova, J., Vorisek, P., Butler, S. (2019). An analysis of trends, uncertainty and  
565 species selection shows contrasting trends of widespread forest and farmland birds in Europe. *Ecol.*  
566 *Indic.* 103, 676–687. DOI: 10.1016/j.ecolind.2019.04.064

567

568 Gröger, J.P., Missong, M., Rountree, R.A. (2011). Analyses of interventions and structural breaks in  
569 marine and fisheries time series: Detection of shifts using iterative methods. *Ecol. Indic.*, 11, 1084–  
570 1092. DOI: 10.1016/j.ecolind.2010.12.008

571

572 Hallmann, C.A., Sorg, M., Jongejans, E., Siepel, H., Hofland, N., Schwan, H., ... Hörren, T. (2017).  
573 More than 75 percent decline over 27 years in total flying insect biomass in protected areas. *PloS*  
574 *One*, 12(10), e0185809. DOI: 10.1371/journal.pone.0185809

575

576 Heldbjerg, H., Sunde, P., Fox, A.D. (2018). Continuous population declines for specialist farmland  
577 birds 1987-2014 in Denmark indicates no halt in biodiversity loss in agricultural habitats. *Bird*  
578 *Conserv. Int.*, 28(2), 278–292. DOI: 10.1017/S0959270916000654

579

580 Humbert, J.-Y., Scott Mills, L., Horne, J.S., Dennis, B. (2009). A better way to estimate population  
581 trends. *Oikos*, 118(12), 1940–1946. DOI: 10.1111/j.1600-0706.2009.17839.x

582

583 Inger, R., Gregory, R., Duffy, J.P., Stott, I., Voříšek, P., Gaston, K.J. (2014). Common European  
584 birds are declining rapidly while less abundant species' numbers are rising. *Ecol. Lett.*, 18(1), 28–  
585 36. DOI: 10.1111/ele.12387

586

587 Jiguet, F., Gadot, A.-S., Julliard, R., Newson, S.E., Couvet, D. (2007). Climate envelope, life history  
588 traits and the resilience of birds facing global change. *Glob. Chang. Biol.*, 13(8), 1672–1684. DOI:  
589 10.1111/j.1365-2486.2007.01386.x  
590

591 Julliard, R., Jiguet, F., Couvet, D. (2004). Common birds facing global changes: what makes a  
592 species at risk? *Glob. Chang. Biol.*, 10(1), 148–154. DOI: 10.1046/j.1529-8817.2003.00723.x  
593

594 Koleček, J., Schleuning, M., Burfield, I.J., Báldi, A., Böhning-Gaese, K., Devictor, V., ... Hnatyna,  
595 O. (2014). Birds protected by national legislation show improved population trends in Eastern  
596 Europe. *Biol. Conserv.*, 172, 109–116. DOI: 10.1016/j.biocon.2014.02.029  
597

598 Koschová, M., Rivas-Salvador, J., Reif, J. (2018). Continent-wide test of the efficiency of the  
599 European union’s conservation legislation in delivering population benefits for bird species. *Ecol.*  
600 *Indic.*, 85, 563–569. DOI: 10.1016/j.ecolind.2017.11.019  
601

602 Link, W.A., Sauer, J.R. (1997a). New approaches to the analysis of population trends in land birds:  
603 comment. *Ecology*, 78(8), 2632–2634. DOI: 10.2307/2265922  
604

605 Link, W.A., Sauer, J.R. (1997b). Estimation of population trajectories from count data. *Biometrics*,  
606 488–497. DOI: 10.2307/2533952  
607

608 Lister, B.C., Garcia, A. (2018). Climate-driven declines in arthropod abundance restructure a  
609 rainforest food web. *Proc. Natl. Acad. Sci. U.S.A.*, 115(44), E10397–E10406. DOI:  
610 10.1073/pnas.1722477115  
611

612 Loh, J., Green, R.E., Ricketts, T., Lamoreux, J., Jenkins, M., Kapos, V., Randers, J. (2005). The  
613 Living Planet Index: using species population time series to track trends in biodiversity. *Philos.*  
614 *Trans. Royal Soc. B-Biol. Sci.*, 360(1454), 289-295. DOI: 10.1098/rstb.2004.1584  
615

616 Mace, G.M., Collen, B., Fuller, R.A., Boakes, E.H. (2010). Population and geographic range  
617 dynamics: implications for conservation planning. *Philos. Trans. Royal Soc. B-Biol. Sci.*,  
618 365(1558), 3743–3751. DOI: 10.1098/rstb.2010.0264  
619

620 Male, T.D., Bean, M.J. (2005). Measuring progress in US endangered species conservation. *Ecol.*  
621 *Lett.*, 8(9), 986–992. DOI: 10.1111/j.1461-0248.2005.00806.x  
622

623 MNHN (2019). Data accessible at [http://www.vigienature.fr/fr/page/produire-des-indicateurs-partir-  
des-indices-des-especes-habitat](http://www.vigienature.fr/fr/page/produire-des-indicateurs-partir-<br/>624 des-indices-des-especes-habitat))  
625

626 Muggeo, V.M. (2003). Estimating regression models with unknown break-points. *Stat. Med.*,  
627 22(19), 3055–3071. DOI: 10.1002/sim.1545  
628

629 Muggeo, V.M. (2008). Segmented: an R package to fit regression models with broken-line  
630 relationships. *R News*, 8(1), 20–25.  
631

632 Narula, S.C. (1979). Orthogonal polynomial regression. *Int. Stat. Rev.*, 31–36. DOI:  
633 10.2307/1403204  
634

635 Newton, I. (2004). The recent declines of farmland bird populations in Britain: an appraisal of  
636 causal factors and conservation actions. *Ibis*, 146(4), 579–600. DOI: 10.1111/j.1474-  
637 919X.2004.00375.x  
638

639 O’neill, B. (2006). *Elementary differential geometry*. Elsevier.  
640

641 Pereira, H.M., Cooper, H.D. (2006). Towards the global monitoring of biodiversity change. *Trends*  
642 *Ecol. Evol.*, 21(3), 123–129. DOI: 10.1016/j.tree.2005.10.015  
643

644 Reif, J. (2013). Long-term trends in bird populations: a review of patterns and potential drivers in  
645 North America and Europe. *Acta ornithol.*, 48(1), 1–16. DOI: 10.3161/000164513X669955  
646

647 Reif, J., Vermouzek, Z. (2019). Collapse of farmland bird populations in an Eastern European  
648 country following its EU accession. *Conserv. Lett.*, 12(1), e12585. DOI: 10.1111/conl.12585  
649

650 Ripple, W.J., Wolf, C., Newsome, T.M., Galetti, M., Alamgir, M., Crist, E., ... Laurance, W.F., 15,  
651 364 scientist signatories from 184 countries (2017). World scientists’ warning to humanity: A  
652 second notice. *BioScience* 67(12), 1026–1028. DOI: 10.1093/biosci/bix125  
653

654 Rodionov, S., Overland, J.E. (2005). Application of a sequential regime shift detection method to  
655 the Bering Sea ecosystem. *ICES J. Mar. Sci.*, 62(3), 328–332. DOI: 10.1016/j.icesjms.2005.01.013  
656

657 Rosenberg, K.V., Dokter, A.M., Blancher, P.J., Sauer, J.R., Smith, A.C., Smith, P.A., Stanton, J.C.,  
658 Panjabi, A., Helft, L., Parr, M. (2019). Decline of the North American avifauna. *Science* 366, 120–  
659 124. DOI: 10.1126/science.aaw1313  
660

661 Ruppert, D., Wand, M.P., Carroll, R.J. (2009). Semiparametric regression during 2003–2007.  
662 *Electron. J. Stat.*, 3, 1193. DOI: 10.1214/09-EJS525  
663

664 Sánchez-Bayo, F., Wyckhuys, K.A. (2019). Worldwide decline of the entomofauna: A review of its  
665 drivers. *Biol. Conserv.*, 232, 8–27. DOI: 10.1016/j.biocon.2019.01.020  
666

667 Sanderson, F.J., Pople, R.G., Ieronymidou, C., Burfield, I.J., Gregory, R.D., Willis, S.G., ... Donald,  
668 P.F. (2016). Assessing the performance of EU nature legislation in protecting target bird species in  
669 an era of climate change. *Conserv. Lett.*, 9(3), 172–180. DOI: 10.1111/conl.12196  
670

671 Schmeller, D. S., Weatherdon, L. V., Loyau, A., Bondeau, A., Brotons, L., Brummitt, N., ... Mihoub,  
672 J. B. (2018). A suite of essential biodiversity variables for detecting critical biodiversity change.  
673 *Biol. Rev.*, 93(1), 55-71. DOI: 10.1111/brv.12332  
674

675 Smith, A.C., Hudson, M.-A.R., Downes, C.M., Francis, C.M., 2015. Change points in the  
676 population trends of aerial-insectivorous birds in North America: synchronized in time across  
677 species and regions. *PLoS One* 10(7). DOI: 10.1371/journal.pone.0130768  
678

679 Soldaat, L.L., Pannekoek, J., Verweij, R.J., van Turnhout, C.A., van Strien, A.J. (2017). A Monte  
680 Carlo method to account for sampling error in multi-species indicators. *Ecol. Indic.* 81, 340–347.  
681 DOI: 10.1016/j.ecolind.2017.05.033  
682

683 Sonali, P., Kumar, D.N. (2013). Review of trend detection methods and their application to detect  
684 temperature changes in India. *J. Hydrol.*, 476, 212–227. DOI: 10.1016/j.jhydrol.2012.10.034  
685

686 Thomas, L. (1996). Monitoring long-term population change: why are there so many analysis  
687 methods? *Ecology*, 77(1), 49–58. DOI: 10.2307/2265653

688

689 Tittensor, D.P., Walpole, M., Hill, S.L., Boyce, D.G., Britten, G.L., Burgess, N.D., Butchart, S.H.,  
690 Leadley, P.W., Regan, E.C., Alkemade, R. (2014). A mid-term analysis of progress toward  
691 international biodiversity targets. *Science* 346, 241–244. DOI: 10.1126/science.1257484

692

693 Vačkář, D., ten Brink, B., Loh, J., Baillie, J. E., Reyers, B. (2012). Review of multispecies indices  
694 for monitoring human impacts on biodiversity. *Ecol. Indic.*, 17, 58-67. DOI:  
695 10.1016/j.ecolind.2011.04.024

696

697 Vasilakopoulos, P., Maravelias, C.D., Tserpes, G. (2014). The alarming decline of Mediterranean  
698 fish stocks. *Curr. Biol.*, 24(14), 1643–1648. DOI: 10.1016/j.cub.2014.05.070

699

700 Vorisek, P., Jiguet, F., Klva, A., Gregory, R.D. (2010). Trends in abundance and biomass of  
701 widespread European farmland birds: how much have we lost? *BOU Proc., Lowland Farmland*  
702 *Birds III*, 1-24.

703

704 Wolkovich, E.M., Cook, B.I., McLauchlan, K.K., Davies, T.J. (2014). Temporal ecology in the  
705 Anthropocene. *Ecol. Lett.*, 17(11), 1365–1379. DOI: 10.1111/ele.12353

706

707 Wood, S.N. (2017). *Generalized additive models: an introduction with R*. Chapman and Hall/CRC.

708

709 Yue, S., Wang, C. (2004). The Mann-Kendall test modified by effective sample size to detect trend  
710 in serially correlated hydrological series. *Water resour. Manag.*, 18(3), 201–218. DOI:  
711 10.1023/B:WARM.0000043140.61082.60

Figures

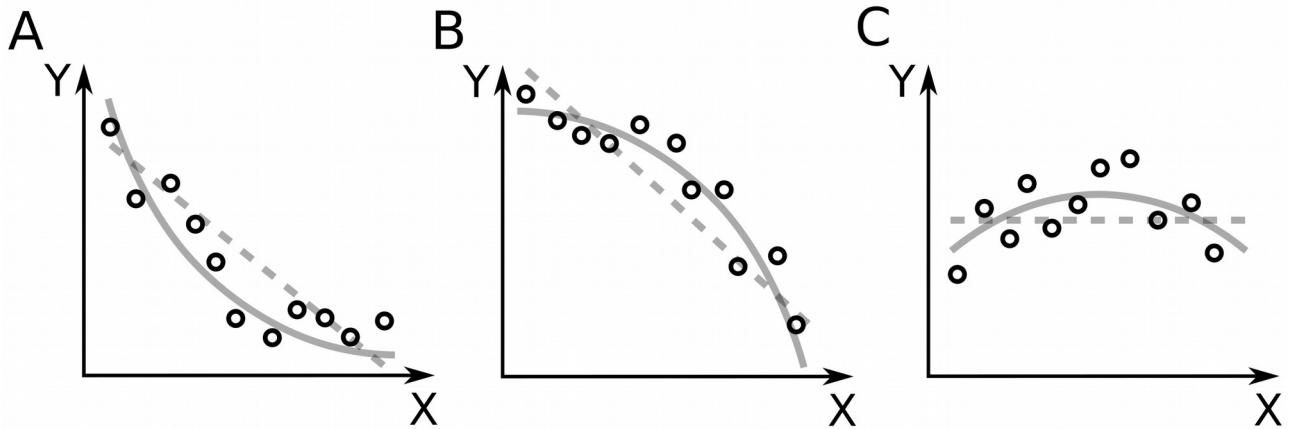


Figure 1: Illustrations of second order polynomial (solid line) and linear (dotted line) fits of  $Y$  (a hypothesised ecological variable (black circles)) by  $X$  (in units of time). A) Second order polynomial fit captures a decelerated decline whereas the linear fit does not. B) Second order polynomial fit captures an accelerated decline whereas the linear fit does not. C) Second order polynomial fit captures a concave phase whereas the linear fit is flat.



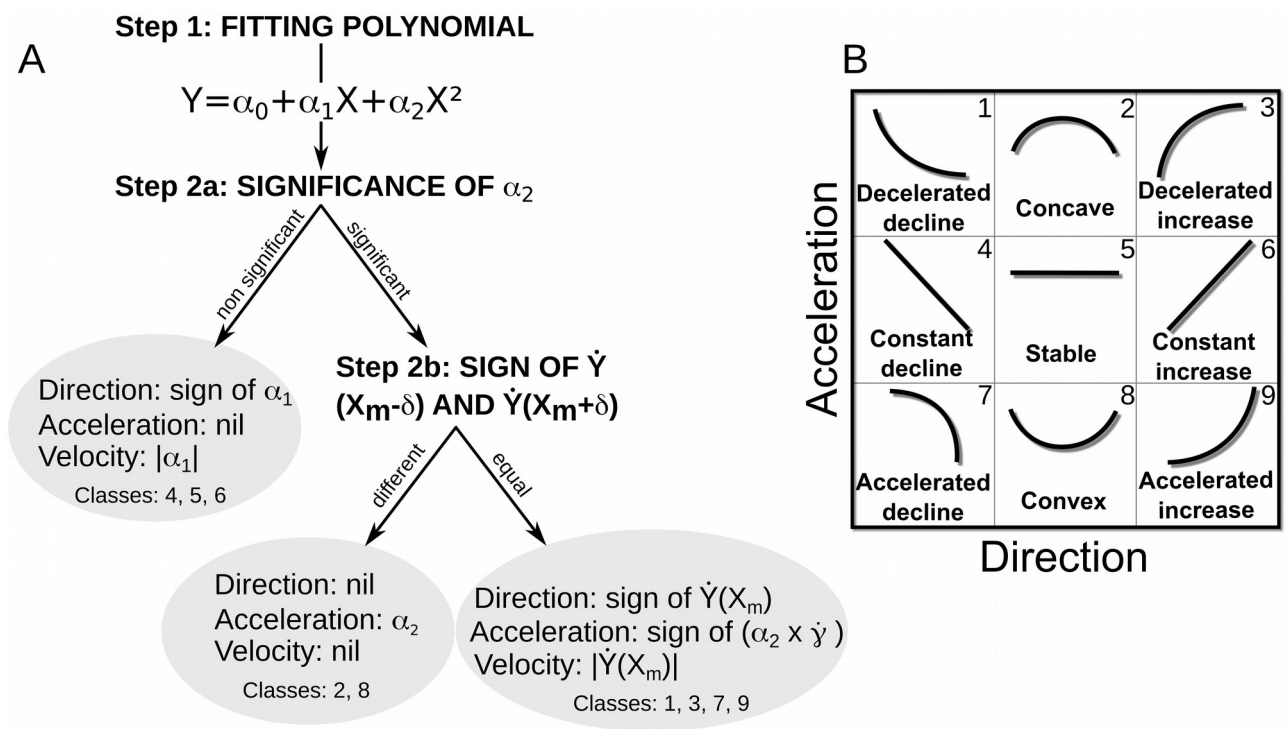


Figure 2: Classification steps (A) and classes (B). Once the second order polynomial  $Y = \alpha_0 + \alpha_1 X + \alpha_2 X^2$  is fitted (step 1), the significance of  $\alpha_2$  is evaluated (step 2a) to distinguish between linear (B. 4, 5 and 6) and non-linear (1, 2, 3, 7, 8 and 9) trajectories. For linear cases, assessing direction and velocity is straightforward using the coefficient of the slope  $\alpha_1$ . For non-linear dynamics (step 2b), concave and convex cases (B. 2 and 8) can be discriminated by a change in the sign of the tangent around  $X_m$ . Remaining classes (1, 3, 7 and 9) require the calculation of the curvature derivative at  $X_m$  as a proxy of the acceleration as well as the computation of the tangent value at  $X_m$  for velocity estimation. B) Class numbering refers to the following types: accelerated decline (1), concave (2), accelerated increase (3), constant decline (4), stable (5), constant increase (6), decelerated decline (7), convex (8), and decelerated increase (9).

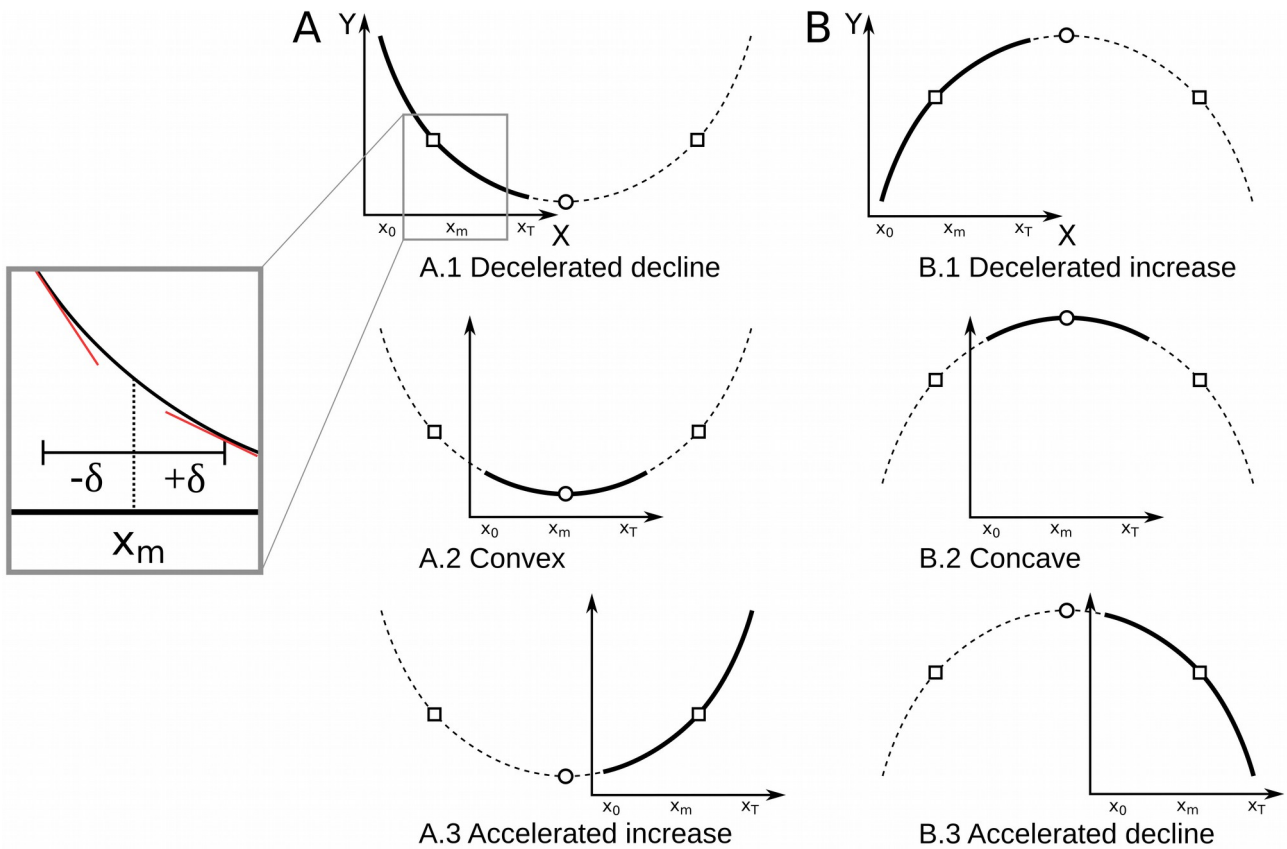


Figure 3: Second order polynomial curves on the time interval  $[X_0, X_T]$ ,  $X_m$  being the middle of the interval. For a given second order polynomial function  $Y = \alpha_0 + \alpha_1 X + \alpha_2 X^2$ , six cases may be described depending on the position of the curve relative to the interval  $[X_0, X_T]$ . For a convex function (A), three cases can be found: a decelerated decline (A.1), a convex phase (A.2), or an accelerated increase (A.3). For a concave function (B), three cases as well can be identified: a decelerated increase (B.1), a concave phase (B.2) or an accelerated decline (B.3). The direction of the trajectory is assessed based on the sign of the tangents at points  $X_m - \delta$  and  $X_m + \delta$  (inset window). Changing points are marked with a circle for  $p_1$  and a square for  $p_2$  and  $p_3$ .  $p_1$  is the point where the tangent becomes zero and delineated increase and decline.  $p_2$  and  $p_3$  are points where the tangent coefficient is 1 or -1. They define where the tangent becomes more horizontally or vertically led.

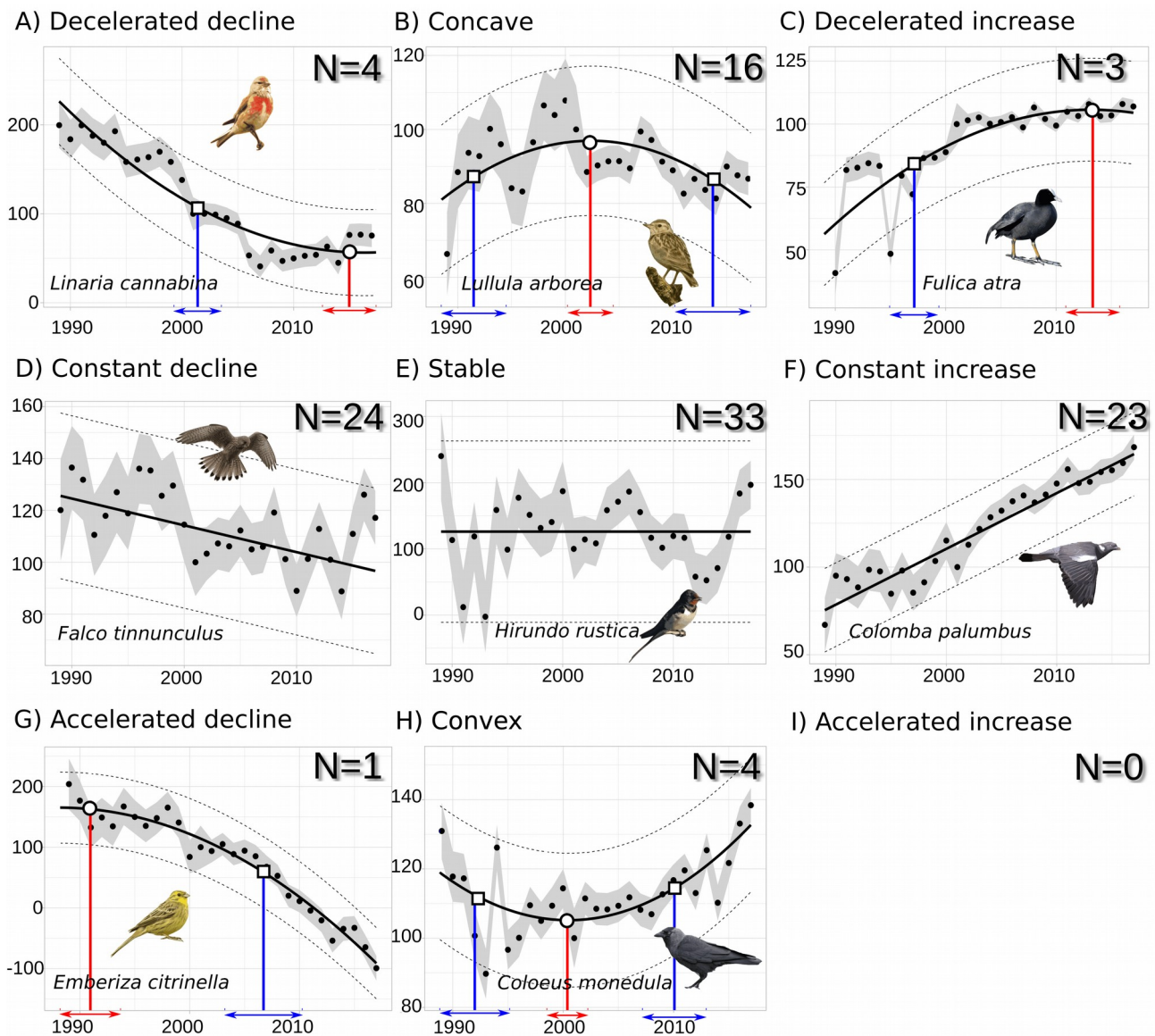


Figure 4: Classification of the 108 bird species trajectories (standardised abundances) from 1989 to 2017 into the nine possible linear (D, E, F) and non-linear (A, B, C, G, H, I) classes. A) 1 accelerated declines, B) 4 concave trajectories, C) 0 accelerated increase, D) 24 constant declines, E) 33 stable trajectories, F) 23 constant increases, G) 4 decelerated declines, H) 16 concave trajectories, I) 3 decelerated increases. Scaled yearly indices of abundance (black dots) with sampling error (grey intervals) are shown for one species of each class. Second order polynomials are shown by a bold line and standard deviations by dashed lines. Changing points of interest are marked on these fits with their standard deviation (bounded segments) (circle and red for  $p_1$  and square and blue for  $p_2$  and  $p_3$ ).

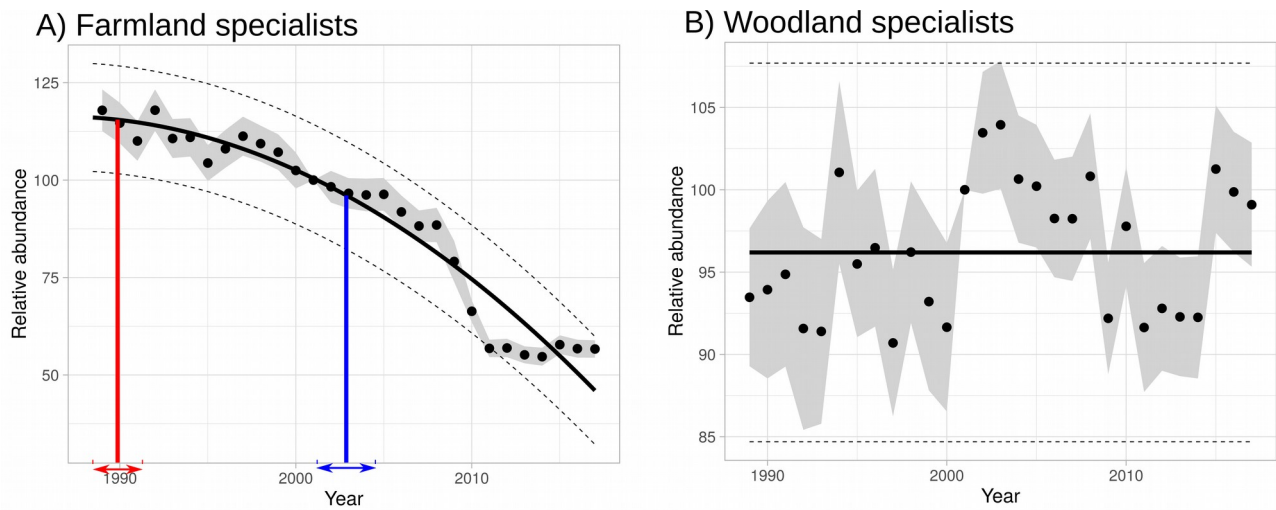


Figure 5: Multi-species indicators (yearly values (black dots) with standard deviation (grey intervals)) of farmland (A) and forest (B) specialist species between 1989 and 2017. A) The second order polynomial is shown by a bold line and standard deviation by dashed lines. Changing point of interest is marked on this fit with its standard deviation (bounded segment) (square and blue for  $p_3$ ). B) A stable fit is represented (bold line and standard deviation by dashed lines) as no linear trend nor second order polynomials were detected.